This is a repository copy of *An emergent optimal resource allocation for climate resilience of transport infrastructure networks*.

White Rose Research Online URL for this paper:
https://eprints.whiterose.ac.uk/227356/

Version: Published Version

**Article:**

Li, Q., Arbabi, H. and Punzo, G. orcid.org/0000-0003-4246-9045 (2025) An emergent optimal resource allocation for climate resilience of transport infrastructure networks. Proceedings of the Royal Society A: Mathematical, Physical and Engineering Sciences, 481 (2317). 20250084. ISSN 1364-5021

https://doi.org/10.1098/rspa.2025.0084

**Reuse**

This article is distributed under the terms of the Creative Commons Attribution (CC BY) licence. This licence allows you to distribute, remix, tweak, and build upon the work, even commercially, as long as you credit the authors for the original work. More information and the full terms of the licence here: https://creativecommons.org/licenses/

**Takedown**

If you consider content in White Rose Research Online to be in breach of UK law, please notify us by emailing eprints@whiterose.ac.uk including the URL of the record and the reason for the withdrawal request.

eprints@whiterose.ac.uk
https://eprints.whiterose.ac.uk/

PROCEEDINGS A

royalsocietypublishing.org/journal/rspa

Downloaded from https://royalsocietypublishing.org/ on 14 July 2025

Research

**Cite this article:** Li Q, Arbabi H, Punzo G. 2025 An emergent optimal resource allocation for climate resilience of transport infrastructure networks. *Proc. R. Soc. A* **481**: 20250084. https://doi.org/10.1098/rspa.2025.0084

Received: 28 January 2025
Accepted: 2 June 2025

**Subject Areas:**
mathematical modelling, civil engineering, computer modelling and simulation

**Keywords:**
resilience, extreme climate change, transport infrastructure, network modelling

**Author for correspondence:**
Giuliano Punzo
e-mail: g.punzo@sheffield.ac.uk

# An emergent optimal resource allocation for climate resilience of transport infrastructure networks

Qianqian Li[1], Hadi Arbabi[1] and Giuliano Punzo[2]

[1]School of Mechanical, Aerospace, and Civil Engineering, and
[2]School of Electrical and Electronic Engineering, University of Sheffield, Sheffield, UK

HA, 0000-0001-8518-9022; GP, 0000-0003-4246-9045

Current infrastructure networks must be climate resilient to continue meeting service demand into the next decades with climate change rapidly pushing infrastructure assets towards or beyond their initial design envelope. At system level, this corresponds to the ability to deliver services when parts of the infrastructure become isolated following local asset failures. Local shielding strategies are typically formulated using abstract network metrics or global optimization methods. The former are agnostic to the specificity of infrastructure systems, while the latter tend to be hardly scalable for large infrastructure networks. Here, we develop an optimal limited-resource allocation strategy to increase network resilience, combining the input sparsity of abstract network metrics with transparency of optimization methods. We focus on transport networks and maximizing the expected throughput of services. We consider upgrading costs as proportional to the desired increase in failure load from climate shocks. We benchmark our method by applying it to the UK freight railway considering shocks induced by an end-of-century RCP8.5 climate change scenario. A closed-form solution naturally emerges for the ranking of the network assets that allows for optimal distribution of limited asset reinforcement investments. We show that this attains better resilience improvements compared to existing heuristic global optimization methods.

Electronic supplementary material is available online at https://doi.org/10.6084/m9.figshare.c.7879893.

© 2025 The Authors. Published by the Royal Society under the terms of the Creative Commons Attribution License http://creativecommons.org/licenses/by/4.0/, which permits unrestricted use, provided the original author and source are credited.

THE ROYAL SOCIETY PUBLISHING

Downloaded from https://royalsocietypublishing.org/ on 14 July 2025

## 1. Introduction

As a changing climate poses an increasing challenge for all infrastructure sectors [1], early climate change adaptation investments have been identified as economically efficient in the long term [2]. The Intergovernmental Panel on Climate Change sixth assessment report defines climate change adaptation as acts that *moderate harm or take advantage of beneficial opportunities*. With mitigation efforts stalling, adaptation is becoming increasingly more crucial in managing the effects of climate change [3].

Recognizing the importance of high-quality infrastructure in economic growth and the risks posed by climate change, national governments have started setting out long-term infrastructure investment plans. As an example, the UK Government has committed to an annualized investment of 1.1–1.3% of the GDP to deliver such infrastructure development plans over the next 30 years [4,5]. The US Bipartisan infrastructure plan proposes $400bn to repair road and bridge infrastructures, where it is estimated that one mile in every five is in poor condition. Moreover, it announced a $50bn investment to increase climate change resilience [6]. However, with limited resources made available to develop and upgrade infrastructure systems, the challenge shifts to how interventions should be prioritized and, consequently, resources should be allocated to minimize future service disruptions [7].

Similar questions of limited resource allocation and resilience have been explored by disciplinary work in network science and operation research. In the context of network science, local metrics have been developed to measure the importance of each node or edge to the structure of the overall system and the effect they may have on altering the dynamics playing out over the system in terms of their contribution to system resilience and their susceptibility to faults and failures. Among the various metrics studied in the literature, those related to *centrality* and *clustering* are recognized as the most fundamental and frequently used local network metrics [8]. Node degree is one of the most intuitive measures for centrality of an asset and its importance [9]. Nodes with a higher degree, i.e. more connected edges, are structurally more crucial than nodes with fewer attached edges. Removing a high-degree node could remove a substantial proportion of edges in the network and is more likely to fragment the original network into two or more disconnected subnetworks. The *betweenness* centralities are a broader family of measures characterizing the importance of nodes or edges in allowing access between other assets in a network [9]. Nodes and edges are considered in a central position if they fall within the shortest path connecting many other node pairs [10]. Their betweenness centrality directly indicates the magnitude of potential disruptions, and if they are to fail. (As both nodes and edges can fail in infrastructure networks, we shall refer to either as assets, meaning lines, junctions, etc.) High betweenness centrality of an asset could indicate a bottleneck between two components or parts of an infrastructure network. Disruptions to such assets are more likely to increase the distance between the unaffected assets, if not entirely disconnect them. In physical infrastructure systems, prioritizing and protecting assets of a higher centrality can be used to avoid failures that could cause larger-scale service disruptions. Clustering, meanwhile, describes the local connectedness of assets in a wider community of nodes, originating in social network studies as cliques, where common friends of a person tend to directly know one another as well [11]. In the context of infrastructure systems, clustering for an asset reflects the likelihood that its immediate neighbours will remain closely connected in the event of its failure [12]. These metrics are often developed with abstract networks in mind and rely solely on topological information to quantify the importance of network assets. Isolated use of such metrics, however, captures insufficient information with respect to a system's unique dynamics and needs to be modified with infrastructure-specific information when inferring components' susceptibility to failure when exposed to external shocks [13–16].

In the context of operation research, a mathematical or computational formulation abstracts the infrastructure system under study and its operation to be then considered within objective functions related to the system's health, safety, functionality, reliability or resilience. With the resource input into the system acting as one of the constraints, the optimization process then seeks

Downloaded from https://royalsocietypublishing.org/ on 14 July 2025

to minimize or maximize the desired function over a feasible set of solutions. These approaches directly solve an explicit formulation of the *problem*, i.e. where/how to allocate a finite set of resources. Objective functions formulated in such cases cover various aspects of infrastructure operations at different levels and are often formulated as functions of the quality of service provided [17,18]. The nature of the system under study is a leading factor in choosing which function to use. Each infrastructure sector has its own performance measures to quantify the service provided, e.g. minimization of the passenger waiting time for public transport systems [19–21]. Optimization models are developed to effectively allocate limited budgets and resources to maintain and improve the overall condition of the network. From the perspective of proactive or reactive actions, pre-disaster resource allocation strategies for resilience look at allocating resources to reinforce the infrastructure system so that the onset effect of disruptive events can be minimized [22–26].

It is clear that topological measures on their own are not universally sufficient for addressing resource allocation problems across infrastructure systems. Objective functions tailored to specific infrastructure systems, which combine topological and functional importance of network assets, are also difficult to generalize. What is needed is a clear mechanism or framework that explains how local asset-level topological metrics are related to the network-level resilience. In this work, we present a generalized analytical solution for resource allocation that, inspired by a linear programming approach, produces a network metric, which naturally ranks both nodes and edges of a flow-centric network based on their contribution to the resilience of the whole system. While the method is easily generalizable, we concentrate on transport system weather resilience and offer a case study on the UK rail network considering the effect of increasing temperatures, as derived from an end-of-century RCP8.5 climate change scenario. We show how our method, which can be applied iteratively for greater accuracy, surpasses the performance of a particle swarm optimization (PSO) while reducing the computational burden.

The rest of this paper is structured as follows: in §2 we offer the formulation of the limited resource allocation problem; we then present an exact analytic solution for a toy model network in §3, leading to the more general formulation. The result, then applied and benchmarked on the UK rail network, is described in §4, allowing us to discuss our findings and offer our conclusions in §§5 and 6.

## 2. A generalized mobility infrastructure network model

We model the infrastructure system as a multilayer network, consisting of a service layer and one or more asset layers. We consider the ultimate purpose of an infrastructure system to be the provision of a service or set of services. It follows that resilience is defined as the ability to maintain the delivery of the services when the system is subject to external shocks [27]. In the context of infrastructure systems/services subject to climate change-related hazards, the successful delivery of a unit service can sometimes rely on multiple interdependent infrastructure systems. Components in each of these systems can be affected by different types of climatic hazards. By separating the service and asset layers, we quantify the scale of disruptions to services as assets fail. With such a separation, it is also possible to incorporate multiple asset layers, which are exposed to different climate hazards, into the assessment.

While amenable to multiple asset layers, our formulation is presented with just one such layer and one service layer, indicated by subscripts $\alpha$ and $\phi$, respectively. Hence, for the asset layer, assets can be thought of as a graph $\mathcal{G}_\alpha = \{\mathcal{V}_\alpha, \mathcal{E}_\alpha\}$, where $\mathcal{V}_\alpha$ and $\mathcal{E}_\alpha$ indicate the set of nodes and edges, respectively. The framework does not need to differentiate node assets and edge assets rigidly; $\mathcal{A}$ indicates the set of assets in layer $\alpha$, with elements $\mathcal{A}_i$, $i = 1, 2, \ldots, |\mathcal{V}_\alpha| + |\mathcal{E}_\alpha|$, with $|\cdot|$ indicating the cardinality of a set. The equivalent definitions for the flow layer $\phi$ are omitted for brevity. We consider a multilayer network with an asset layer, $\mathcal{G}_\alpha = \{\mathcal{V}_\alpha, \mathcal{E}_\alpha\}$, and an origin–destination (OD) layer $\mathcal{G}_\phi = \{\mathcal{V}_\phi, \mathcal{E}_\phi\}$, as services. The asset layer represents the network of the physical assets in the infrastructure system, such as stations and railway lines. The flow layer

Downloaded from https://royalsocietypublishing.org/ on 14 July 2025

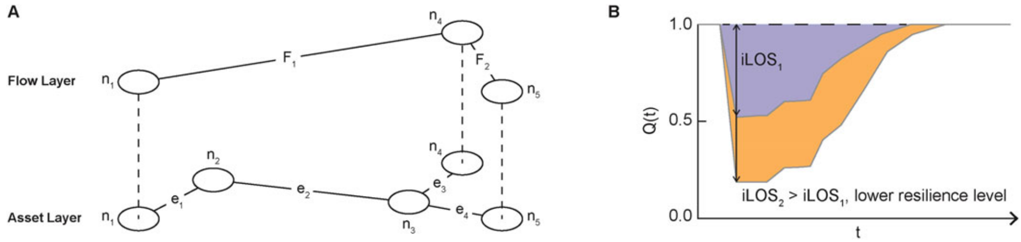


**Figure 1.** A simple network illustration for the bi-layer structure (A) and a schematic resilience curve with loss of service highlighted (B)—adapted from [28].

represents the service provided by the infrastructure system, such as transporting passengers and commodities.

The node set of the OD layer is a subset of the asset layer, $\mathcal{V}_\phi \in \mathcal{V}_\alpha$, including the origin and destination nodes and excluding some intermediate connection nodes. The edge sets of the two layers are two separate sets, $\mathcal{E}_\phi \notin \mathcal{E}_\alpha$. Each OD pair is assumed to have one specific route in the asset layer in our network model. Moving commodities from an origin node to a destination node requires all track segments along the route to be in working condition. Hence, an *OD pair* refers to an edge in the flow layer and an *OD path* refers to an ordered list of edges in the asset layer that the OD pair relies on to deliver the OD flow.

This dependent relationship between the asset layer and the flow layer is captured by a link-route incidence matrix $H$. The number of rows in $H$ equals the number of edges in the asset layer and the number of columns equals the number of OD pairs in the flow layer. Therefore, $H$ is of size $|\mathcal{E}_\alpha| \times |\mathcal{E}_\phi|$ and $H_{i,j} = 1$ denotes that edge $e_i \in \mathcal{E}_\alpha$ belongs to the OD path of OD pair $OD_j \in \mathcal{E}_\phi$; otherwise $H_{i,j} = 0$. In the simple network illustrated in figure 1A, OD flow $F_1$ relies on edges $e_1$, $e_2$ and $e_3$ in the asset layer, while OD flow $F_2$ relies on edges $e_3$ and $e_4$. This corresponds to a link-route incidence matrix for the simple network:

$$H = \begin{array}{c} \\ e_1 \\ e_2 \\ e_3 \\ e_4 \end{array} \begin{array}{c} \begin{array}{cc} F_1 & F_2 \end{array} \\ \begin{bmatrix} 1 & 0 \\ 1 & 0 \\ 1 & 1 \\ 0 & 1 \end{bmatrix} \end{array}.$$

The resilience of infrastructure systems often spans from robustness, the ability to resist and absorb external shocks, to recoverability, the ability to restore services quickly [29,30]. When plotted against time, the loss and gradual recovery of services produce a triangular shape in the time history of the system key performance parameters, against which its resilience is considered (e.g. [31]). The area of such a triangle, which is also the cumulative loss of service, when the performance considered, is the overall service provision, and primarily depends on the scale of the initial disruption (drop in services, measured along the vertical axis) and time taken to restore full functionality, figure 1B.

Here, we consider minimizing the initial disruption, which ultimately leads to a minimized cumulative service loss. Therefore, the objective function for the optimization problem can be minimizing the initial loss of service, $Q(t = 0)$, or maximizing the amount of remaining service, $1 - Q(t = 0)$, where $t = 0$ refers to the time a disruptive event occurs. For a given climatic condition, $\omega$, each edge asset $i$ is given a local load variable in the set $\boldsymbol{\omega} = \{\omega_i, \dots \omega_\alpha\}$, where $i = 1, 2, \dots |\mathcal{E}_\alpha|$.

A fragility function, here taken in the form of the cumulative density function of the standard normal distribution, maps the local weather parameter, $\omega_i$, to the probability of failure for asset $e_i$. This captures the non-deterministic relation between an edge exceeding its design load, $\mu_i$, and failing. Safety factors, ageing and maintenance activities contribute to the variance of such a distribution; however, they are difficult to quantify [32]. If the sample size is large enough, the empirical distribution of the true failure load can be described by a normally distributed

Downloaded from https://royalsocietypublishing.org/ on 14 July 2025

random variable, $\Omega \sim \mathcal{N}(\mu_i, \sigma_i)$, where $\sigma_i$ expresses the average difference between the designed and actual failure loads. For a given external weather parameter, $\omega_i$, the probability of failure for edge $e_i$ equals the probability of edges $e_i$ actual failure load being equal or smaller than $\omega_i$, or $p_i = P(\Omega \leq \omega_i)$. Therefore, we take the probability of failure for edge $e_i$ under external weather parameter $\omega_i$ to be

$$p_i = P(\Omega \leq \omega_i) = \frac{1}{2}\left[1 + \text{erf}\left(\frac{\omega_i - \mu_i}{\sigma_i\sqrt{2}}\right)\right], \tag{2.1}$$

where $p_i \in [0, 1]$ is the probability of failure for edge $e_i$; $\omega_i$ could be any weather parameter, e.g. temperature, wind speed or precipitation, and $\mu_i$ and $\sigma_i$ are the shape-control parameters for the fragility function for asset $e_i$ and are also associated with the asset's condition. This choice provides weather-dependent failure scenarios based on the RCP8.5 climate models, after the work in [28]. Note that, intensity, time and spatial extent of extreme heat events are also considered. To develop the resource allocation strategy, the independent variable $\omega_i$ is then sampled from RCP8.5 climate models, considering both average and worst-case day scenarios. This is expanded on further in the case study. Similarly, the design threshold used in the fragility function is related directly and taken from existing studies of heat load effects, based on the work of [33].

The probabilities of individual asset failure can be mapped to the probabilities of OD flow interruption. An OD service path can only be assumed to run successfully when all of its assets function undisrupted. The probability of a service successfully running for an OD path $\text{OD}_j$ equals the combined probability of all of its dependent edges not failing. Therefore, the probability of success for OD path $F_j$ is

$$p(F_j) = \prod_i (1 - H_{i,j}p_i). \tag{2.2}$$

Subsequently, the expected delivery, $E_j$, for OD pair $\text{OD}_j$, can be obtained by multiplying the demand along the OD path for flow $F_j$ with the path's probability of not failing:

$$E_j = F_j \prod_i (1 - H_{i,j}p_i). \tag{2.3}$$

The expected delivery across the whole system is therefore sum of the expected deliveries for all of the OD pairs:

$$\begin{aligned} E &= \sum_j E_j \\ &= \sum_j F_j \prod_i (1 - H_{i,j}p_i) \\ &= \sum_j F_j \prod_i \left(1 - H_{i,j}\frac{1}{2}\left(1 + \text{erf}\left(\frac{\omega_i - \mu_i}{\sigma_i\sqrt{2}}\right)\right)\right). \end{aligned} \tag{2.4}$$

## (a) The resource allocation problem

We shall now find the optimal resource allocation in terms of upgrading efforts to be distributed between infrastructure assets to minimize the system's service disruptions under plausible future extreme weather events.

We assume that edges in the asset layer can be upgraded to a higher design load $\mu_i^*$ from its original design load $\mu_i$ by $\Delta\mu_i$:

$$\mu_i^* = \mu_i + \Delta\mu_i, \tag{2.5}$$

so that failure probability will be reduced when exposed to the same weather parameter:

$$p_i^* = \frac{1}{2}\left(1 + \text{erf}\left(\frac{\omega_i - \mu_i^*}{\sigma_i\sqrt{2}}\right)\right). \tag{2.6}$$

The vector $\boldsymbol{\Delta\mu}$ contains the amount of upgrade $\Delta\mu_i$ for all of the asset:

$$\boldsymbol{\Delta\mu} = \{\Delta\mu_i, \ldots\}, \quad i = 1, 2, \ldots |\mathcal{E}_\alpha|. \tag{2.7}$$

Downloaded from https://royalsocietypublishing.org/ on 14 July 2025

Upon such an upgrade, when the system is subject to the same external weather parameters $\boldsymbol{\omega}$, the expected delivery should now be increased from $E$ to $E^*$. This yields an optimization for an initial loss of services (*iLOS*) that can be expressed as

$$\min_{\boldsymbol{\Delta\mu}} iLOS = \min_{\boldsymbol{\Delta\mu}} \sum_j F_j - E^*$$

$$= \min_{\boldsymbol{\Delta\mu}} \sum_j F_j \left(1 - \prod_i \left(1 - H_{i,j}\frac{1}{2}\left(1 + \mathrm{erf}\left(\frac{\omega_i - (\mu_i + \Delta\mu_i)}{\sigma_i\sqrt{2}}\right)\right)\right)\right), \tag{2.8}$$

subject to

$$\sum_{i=1} c_i \Delta\mu_i = C, \tag{2.9}$$

$$\Delta\mu_i \geq 0, \quad \text{for all } i \tag{2.10}$$

and

$$\Delta\mu_i \leq \Delta\mu_i^{ub}, \quad \text{for all } i. \tag{2.11}$$

Here, the sum of all OD flows, $\sum_j F_j$, is the amount of flows delivered in the network without any asset failures and is a constant given the system's typical overall demand. Such an upgrade would come at a cost $\sum_{i=1} c_i \Delta\mu_i$, where $c_i$ denotes the unit cost to increase the design load of edge $e_i$. The values of $c_i$ could differ from edge to edge depending on asset conditions. The cost of upgrade edge $e_i$ by $\Delta\mu_i$ is simply the product of the unit cost and the amount of increase in the design load, $c_i\Delta\mu_i$.

We consider a finite budget for infrastructure asset upgrades, $C$, made available to the whole system, which can be used for any subsets of assets. The increase in design load is also subject to physical and practical limits [34]. We constrain $\Delta\mu_i$ to an upper bound $\Delta\mu_i^{ub}$ to exclude trivial solutions which are physically inconsistent, and to a zero lower bound assuming that the assets' load capacity can only be increased diminished in their load capacity to invest this elsewhere in the network. Therefore,

## 3. Low-dimensional approach

We shall now concentrate on a three-node, two-edge network and solve the optimal resource allocation model explicitly. The toy model used is shown in figure 2A. We aim at an analytic solution that expresses the optimal resource allocation as a function of the key input variables, that is, the local weather parameters ($\omega$), the assets condition ($\mu$), the unit cost ($c$), the pairwise service demands ($F$) and the link-route incidence matrix ($H$).

The asset layer, figure 2A, has nine nodes and two edges. The service layer comprises three OD pairs. The current design loads are denoted as $\mu_1$ and $\mu_2$ for edge $e_1$ and $e_2$. The fragility function for each edge is

$$p_i(\omega) = \frac{1}{2}\left(1 + \mathrm{erf}\left(\frac{\omega - \mu_i}{\sigma_i\sqrt{2}}\right)\right) \quad i \in \{1, 2\}. \tag{3.1}$$

The flow of services between OD pairs in the service layer is denoted as $F_1, F_2$ and $F_3$. The delivery of $F_1$ from $n_1$ to $n_2$ depends solely on the functioning of $e_1$, and therefore the first column of the route-link incidence matrix, $H$, is $[1, 0]^\top$. The delivery of $F_2$ from $n_1$ to $n_3$ depends on the functioning of $e_1$ and $e_2$ and therefore the second column of H is $[1, 1]^\top$. Similarly, the third column is $[0, 1]^\top$. The route-link incidence matrix is therefore

$$H = \begin{bmatrix} 1 & 1 & 0 \\ 0 & 1 & 1 \end{bmatrix}.$$

In this simple test model, $j \in \{1, 2, 3\}$ as there are three OD flows and $i \in \{1, 2\}$, as there are two edges in the asset layer. The total expected delivery can be calculated as the sum of the OD flows

Downloaded from https://royalsocietypublishing.org/ on 14 July 2025

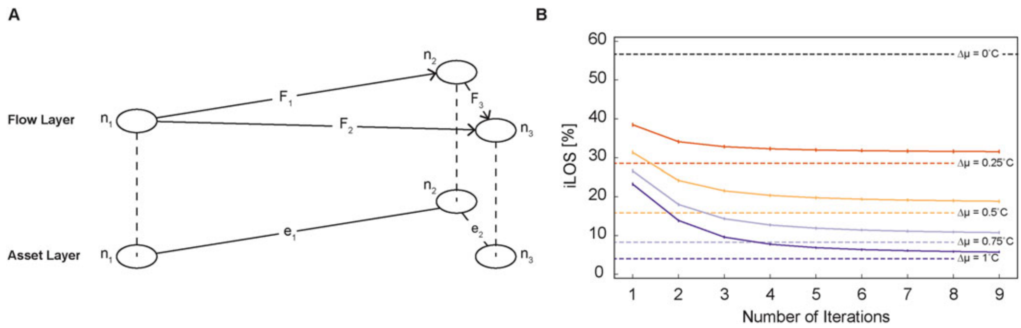


**Figure 2.** The network structure of the test model. The flow layer has three OD pairs. The asset layer is a network of three nodes and three edges.

$F_1$, $F_2$ and $F_3$ multiplied by their corresponding OD path's probability of succeeding. Therefore, expanding equation (2.4), we get

$$E = \sum_j F_j \prod_i (1 - H_{i,j} p_i) \tag{3.2}$$

$$= F_1(1 - H_{1,1}\, p_1)(1 - H_{2,1}\, p_2) + F_2(1 - H_{1,2}\, p_1)(1 - H_{2,2}\, p_2) + F_3(1 - H_{1,3}\, p_1)(1 - H_{2,3}\, p_2). \tag{3.3}$$

Considering the actual elements of H for this network, this becomes

$$\begin{aligned} E &= F_1(1 - p_1) + F_2(1 - p_1)(1 - p_2) + F_3(1 - p_2) \\ &= (F_1 + F_2 + F_3) - p_1(F_1 + F_2) - p_2(F_2 + F_3) + p_1 p_2 F_2. \end{aligned} \tag{3.4}$$

We assume that the edges in the asset layer can be upgraded to higher design loads by an increment of $\boldsymbol{\Delta\mu} = \{\Delta\mu_1, \Delta\mu_2\}$, resulting in reduced probabilities of failure, $p_i^*$ as defined in equation (2.6) for $i = \{1, 2\}$. The expected delivery with the upgrade, $E^*$, is then

$$E^* = (F_1 + F_2 + F_3) - p_1^*(F_1 + F_2) - p_2^*(F_2 + F_3) + p_1^* p_2^* F_2. \tag{3.5}$$

The expected initial loss of service (*iLOS*), figure 1B, at the onset of the disruption without any re-routing or repairing efforts, is

$$\begin{aligned} iLOS &= (F_1 + F_2 + F_3) - E^* \\ &= p_1^*(F_1 + F_2) + p_2^*(F_2 + F_3) - p_1^* p_2^* F_2. \end{aligned} \tag{3.6}$$

In this case, the minimization problem in equation (2.8) can be expressed as

$$\min_{\boldsymbol{\Delta\mu}} iLOS, \tag{3.7}$$

subject to

$$c_1 \Delta\mu_1 + c_2 \Delta\mu_2 = C, \quad \Delta\mu_1 \le \Delta\mu_1^{ub}, \quad \Delta\mu_2 \le \Delta\mu_2^{ub}, \quad \Delta\mu_1 \ge 0, \quad \Delta\mu_2 \ge 0. \tag{3.8}$$

We can write the marginal increments of *iLOS* in response to a change of design threshold from equation (3.6) as

$$A\Delta\mu_1 + B\Delta\mu_2 + D\Delta\mu_1\Delta\mu_2, \tag{3.9}$$

where

$$A = p_1'(F_1 + F_2) - p_2 p_1' F_2, \tag{3.10}$$

$$B = p_2'(F_2 + F_3) - p_1 p_2' F_2 \tag{3.11}$$

and

$$D = -F_2 p_1' p_2', \tag{3.12}$$

Downloaded from https://royalsocietypublishing.org/ on 14 July 2025

with, $p_1', p_2'$ as the derivatives of the probabilities of failure for assets 1 and 2 with respect to the design loads $\mu_1$ and $\mu_2$, respectively, to upgrade. Note that, the problem of minimizing initial loss can equivalently be formulated as maximizing the return of the infrastructure upgrade investment through maximizing the expected additional delivery, subject to the same constraints, see electronic supplementary material, section S1. Rearranging equation (3.10) as $A = p_1'(F_1 + (1 - p_2)F_2)$ provides a more tangible interpretation as it can now be seen as the rate of change of the probability of failure, $p_1'$, multiplied by the amount of flow that is dependent on the success of edge $e_1$.

## (a) Linear programming approach

The Lagrangian for the optimization problem equation (3.7) is defined as

$$\begin{aligned} L(\Delta\mu_1, \Delta\mu_2, \lambda, \theta_1, \theta_2, \varphi_1, \varphi_2) = {} & A\Delta\mu_1 + B\Delta\mu_2 + D\Delta\mu_1\Delta\mu_2 - \lambda(c_1\Delta\mu_1 + c_2\Delta\mu_2 - m(c_1 + c_2)) \\ & - \theta_1(\Delta\mu_1 - \Delta\mu_1^{ub} + t_1^2) - \theta_2(\Delta\mu_2 - \Delta\mu_2^{ub} + t_2^2) \\ & - \varphi_1(\Delta\mu_1 - s_1^2) - \varphi_2(\Delta\mu_2 - s_2^2), \end{aligned} \tag{3.13}$$

where $\lambda, \theta_1, \theta_2, \varphi_1$ and $\varphi_2$ are the Lagrange multipliers and $t_1^2, t_2^2, s_1^2$ and $s_2^2$ are slack variables that are introduced to convert the inequality constrains into equalities. The four inequality constraints mean $2^4 = 16$ cases to discuss. The solution, obtained by taking the gradient of the Lagrangian with respect to each variable is found in each case and is and detailed in the electronic supplementary material, section S2, while here only the solution of unconstrained case is considered as the others present either unrealistic or trivial outcomes.

### (i) Solution of the unconstrained optimization (none of the inequality constrains is active)

We consider $(\theta_1 = 0, t_1^2 > 0), (\theta_2 = 0, t_2^2 > 0), (\varphi_1 = 0, s_1^2 > 0)$ and $(\varphi_2 = 0, s_2^2 > 0)$. The solution can be found by solving

$$\begin{cases} A + D\Delta\mu_2 - \lambda c_1 = 0, \\ B + D\Delta\mu_1 - \lambda c_2 = 0, \\ C - c_1\Delta\mu_1 - c_2\Delta\mu_2 = 0, \end{cases} \tag{3.14}$$

which returns

$$\Delta\mu_1 = \frac{CD + Ac_2 - Bc_1}{2Dc_1} \quad \text{and} \quad \Delta\mu_2 = \frac{CD - Ac_2 + Bc_1}{2Dc_2}. \tag{3.15}$$

Feasibility of the above solution need to be checked with if there exist $t_1^2 > 0, t_2^2 > 0, s_1^2 > 0$ and $s_2^2 > 0$ that satisfy

$$\frac{\partial L}{\partial \theta_1} = \frac{\partial L}{\partial \theta_2} = \frac{\partial L}{\partial \varphi_1} = \frac{\partial L}{\partial \varphi_2} = 0. \tag{3.16}$$

If any of the gradients can not find a slack variable such that the gradient can be zero, the solution from this case will be ruled unfeasible. This situation happens when the solution found in this case turns out to be outside the feasible region defined by the constraints. When there are no constraints considered, the solution calculated with equation (3.15) is the optimal solution. With the presence of the equality and inequality constraints, it could turn out to be an unfeasible solution.

Downloaded from https://royalsocietypublishing.org/ on 14 July 2025

## (b) Generalized approach

The understanding achieved through the low-dimensional approach can now be used to consider the more general case. Rearranging equation (3.15) yields:

$$\left.\begin{aligned} c_1\Delta\mu_1 - \frac{C}{2} &= \frac{c_1c_2}{D}\left(\frac{A}{c_1} - \frac{1}{2}\left(\frac{A}{c_1}+\frac{B}{c_2}\right)\right) \\ \text{and}\qquad c_2\Delta\mu_2 - \frac{C}{2} &= \frac{c_1c_2}{D}\left(\frac{B}{c_2} - \frac{1}{2}\left(\frac{A}{c_1}+\frac{B}{c_2}\right)\right).\end{aligned}\right\} \tag{3.17}$$

It is easy to show that for a constant unit cost $c_1 = c_2 = c$, the optimal level of upgrade is related to the relative value of $A$ and $B$, $\Delta\mu \propto |A - B|$. Consider the generic edge $e_i$ and, without loss of generality, assume $i = 1$ so to link the toy example to the following. From equation (3.17), in the optimized resource allocation solution, the amount of more-than-average resource allocated to edge $e_1$ is a linear function of the difference between $A/c_1$ and the average of $(A/c_1, B/c_2)$. The $(F_1 + (1 - p_2)F_2)$ in $A$ and the $(F_3 + (1 - p_1)F_2)$ in $B$ need to be generalized so that they can be applied to problems with more than two edges. Consider the first edge $e_{i=1}$, the direct sum of the OD flows that use edge $e_1$ is $F_1 = \sum_j H_{1,j}F_j$.

Each of the $F_j$ flows has to be scaled by the probability of failure to calculate the true proportion of $F_j$ that is expected to use edge $e_{i=1}$ through

$$\prod_{k,k\neq 1}(1 - H_{k,j}p_k).$$

Similarly, $A = p_1'(F_1 + (1 - p_2)F_2)$ and $B = p_2'(F_3 + (1 - p_1)F_2)$ are, hence, generalized to

$$p_i'\sum_j H_{i,j}F_j \prod_{k,k\neq i}(1 - H_{k,j}p_k). \tag{3.18}$$

Generalized $A/c_1$ and $B/c_2$ are therefore

$$\frac{p_i'}{c_i}\sum_j H_{i,j}F_j \prod_{k,k\neq i}(1 - H_{k,j}p_k). \tag{3.19}$$

If instead we consider the term for edge $e_i$ from equation (2.3) and extend it to all expected OD flows $E_j$, the total expected delivery across the network $E$ cab be obtained as

$$\begin{aligned} E = \sum_j E_j &= \sum_j\left[(1 - H_{i,j}p_i)F_j \prod_{k,k\neq i}(1 - H_{k,j}p_k)\right] \\ &= \sum_j\left[F_j\prod_{k,k\neq i}(1 - H_{k,j}p_k) - p_i\sum_j H_{i,j}F_j\prod_{k,k\neq i}(1 - H_{k,j}p_k)\right].\end{aligned} \tag{3.20}$$

Differentiating with respect to $\mu_i$ gives the 'gradient', i.e. the change rate of the total expected flow for investing in edge $e_i$:

$$\frac{\partial E}{\partial \mu_i} = -\frac{\partial p_i}{\partial \mu_i}\sum_j H_{i,j}F_j\prod_{k,k\neq i}(1 - H_{k,j}p_k). \tag{3.21}$$

Note that the right-hand side of equation (3.21) matches the generalized analytical solution obtained in equation (3.19) except for the multiplicative term $1/c_i$. This means that the derivative of the expected flow on an edge with respect to the upgrade that the edge receives is proportional to the optimal amount of resources the edge can be allocated.

Downloaded from https://royalsocietypublishing.org/ on 14 July 2025

The term $\partial E/\partial \mu_i$ indicates the gradient of investing in edge $e_i$. Assuming there is a sufficiently small portion, $\Delta\mu_i$ allocated to edge $e_i$, the resulted change in the objective function $\Delta E$ can be approximated as

$$\Delta E = \Delta\mu_i \frac{\partial E}{\partial \mu_i}. \tag{3.22}$$

With the associated cost of upgrading edge $e_i$ by $\Delta\mu_i$ being $\Delta\mu_i c_i$, the true gradient of investing in edge $e_i$ is

$$\frac{\Delta E}{\Delta\mu_i c_i} = \frac{\Delta\mu_i \frac{\partial E}{\partial \mu_i}}{\Delta\mu_i c_i} = -\frac{p_i'}{c_i} \sum_j H_{i,j} F_j \prod_{k,k\neq i} (1 - H_{k,j} p_k). \tag{3.23}$$

A ranking of the assets can then be obtained based on the ability of the asset to contribute to the expected network flow delivery for every unit of resources allocated to their upgrade.

## (c) Ranking strategies

Network resource allocations can often be seen as ranking problems. The underlying assumption is that components of high topological or functional importance, e.g. a vertex with many edges, or an edge that is part of the shortest path of many node pairs, should be prioritized. Node ranking metrics exist that are able to provide measures of individual node and edge importance, offering good computational advantages. Network components of relatively high importance enjoy proportionally large amounts of resources. In a ranking-based resource allocation the amount of upgrade $\Delta\mu_i$ for any edge $e_i$ is proportional to its calculated ranking score $\gamma_i$. Defining $\chi$ as the proportionality constant, for any edge $e_i$ we get

$$\Delta\mu_i = \chi\gamma_i. \tag{3.24}$$

To satisfy the first boundary condition equation (2.9), the total cost of upgrade for all edges needs to equal the given budget, $C$:

$$\sum_i c_i \Delta\mu_i = \sum_i c_i \chi \gamma_i = C. \tag{3.25}$$

Rearranging equation (3.25) and substituting into equation (3.24), the resource allocation solution can be found by calculating each $\Delta\mu_i$ as

$$\Delta\mu_i = \gamma_i \frac{C}{\sum_i c_i \gamma_i}. \tag{3.26}$$

The resource allocation generated this way naturally satisfies the boundary conditions $\sum c_i \Delta\mu_i = C$ and $\Delta\mu_i \geq 0$. The upper boundary constraint can be handled by resetting $\Delta\mu_i$ to $\Delta\mu_i^{ub}$ if $\Delta\mu_i > \Delta\mu_i^{ub}$. This resetting leaves $c_i * (\Delta\mu_i - \Delta\mu_i^{ub})$ amount of resources unused, which can be allocated by running the ranking-based resource allocation again, as in algorithm 1.

However, the ranking metrics available have not been engineered to improve resilience of infrastructure network through local upgrading. Taking the gradient of the expected network flow delivery with respect to the upgrades of the single assets allows us to overcome the generality of the existing ranking metrics. In this way, assets will be ranked based on the cost/benefit balance of investing in them. This is achieved by applying equation (3.21) to all edges. We define this local gradient as the new ranking metric:

$$\gamma_i = \frac{\partial E}{\partial \mu_i} \quad \text{for all } i \in \mathcal{E}_\alpha, \tag{3.27}$$

and we show next how this applies iteratively to a transport network upgrade problem. We define this as the iterative resilience metric-based approach or algorithm (IRMA).

# 4. A case study on the UK railway network

To evaluate the performance of the proposed iterative approach, a system model for this core freight network is constructed, consisting of two layers. The edges in the asset layer represent the

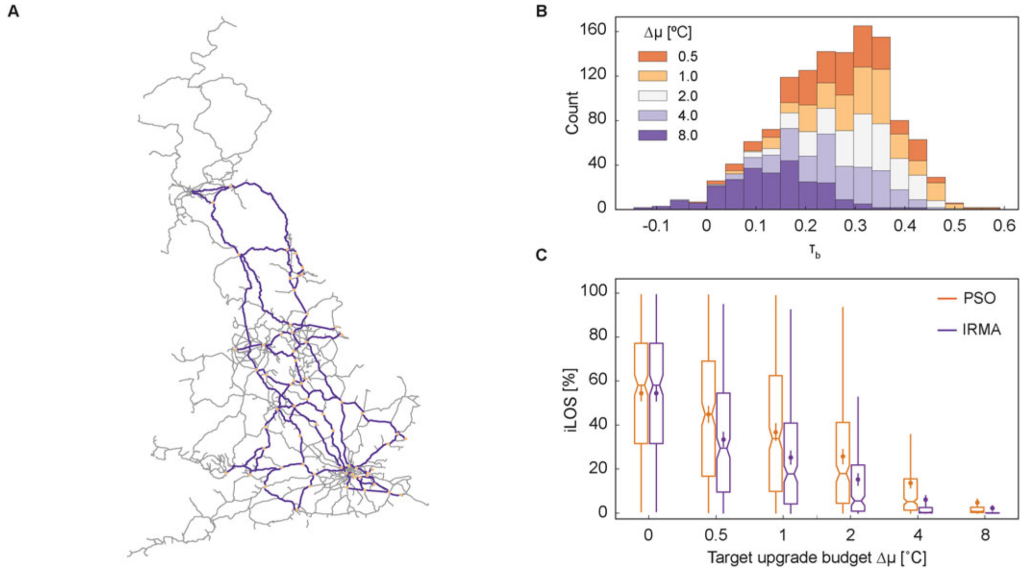


**Figure 3.** The asset layer constructed for this study (purple) as embedded in all railway track lines across the country that are managed by Network Rail (grey) (A). The original shape file is provided by Network Rail. The rankings of the edges to upgrade broadly agree between the PSO and the IRMA (B). Greater agreement occurs when the resources are more scarce while the abundance of resources makes ranking irrelevant. The box plot (C) shows the values attained by the objective function minimized using the PSO algorithm and the proposed metric-based approach with different levels of investment ($\Delta\mu_{eq} \in [0.5, 1, 2, 4, 8]$). The objective function is the expected initial service disruption in percentage of the normal service level for a given weather profile. $\Delta\mu_{eq}$ indicates the investment level. $\Delta\mu_{eq} = 2$ means the amount of investment equals to that required to increase the design load for all assets in the network by 2°C.

railway track lines, figure 3A. The asset layer consists of 65 nodes and 84 edges, which has been constructed based on the maps and descriptions of the freight corridors in the Freight Network Study [35].

The service layer is constructed using the freight train schedule data obtained from the open data feed (openraildata.com, last accessed March 2022) by Network Rail. The constructed service layer has 1623 OD pairs. Converting the station record to node paths in the asset layer, then to edge paths, gives the link-route incidence matrix $H$.

As the downloaded dataset does not include information on the weight or volume of goods transported, loaded and unloaded at each calling station, a scheduled run on a single day is treated as a single unit of flow in the service layer. The total number of runs for each schedule divided by the number of days in the schedule gives the average daily traffic profile. Adding up the trips of all schedules, the simplified location records of which are identical, gives $F$, the amount of flow between the OD pairs. While asset information is not available to inform realistic costs, $\boldsymbol{c}$, this is assumed to be proportional to the geographical length of the edges.

When directly applying the method to the freight network, instead of specifying the number of iterations, $k$, a step size $\Delta\mu(k)$ is specified. In each iteration, the algorithm tries to allocate $\Delta\mu(k)$ amount of resources between edges. The solution obtained will be checked, and where there is a violation of the upper boundary constraint, the value of $\Delta\mu_i$ will be reset to $\Delta\mu_i^{ub}$. The unused resources $c_i * (\Delta\mu_i - \Delta\mu_i^{ub})$ are recycled back to the reservoir of not-yet-allocated resources and are allocated in the following iterations. Note that, $\Delta\mu(k)$ amount of resources are to be allocated at each iteration until less than $\Delta\mu(k)$ resources are left. As the final iteration, the algorithm will then allocate the residual until all resources are used. The pseudo-code explaining the iterative metric-based resource allocation is presented in algorithm 1.

Downloaded from https://royalsocietypublishing.org/ on 14 July 2025

Downloaded from https://royalsocietypublishing.org/ on 14 July 2025

**Algorithm 1:** IRMA

**input :** $\Delta\mu_{eq}$ – total upgrade budget in °C per asset
$\Delta\mu(k)$ – incremental budget available in step $k$
**c** – upgrade unit cost vector
**ub** – asset upgrade upper bound vector in °C
**output:** $\boldsymbol{\Delta\mu}$ – asset upgrade vector in °C
$\boldsymbol{\Delta\mu} \leftarrow 0$;
$\boldsymbol{\gamma} \leftarrow \frac{\partial E}{\partial \mu}$;
utilizationRatio $\leftarrow \frac{\boldsymbol{\Delta\mu}^\top \mathbf{c}}{\Delta\mu_{\text{eq}}}$;
**while** utilizationRatio $< 1$ **do**
  $\Delta\mu_{\text{remaining}} \leftarrow (1 - \text{utilizationRatio})\Delta\mu_{\text{eq}}$;
  $\Delta\mu(k) \leftarrow \min\{\Delta\mu_{\text{remaining}}, \Delta\mu(k)\}$;
  **if** $\Delta\mu_i + \gamma_i \frac{\Delta\mu(k)}{\mathbf{c}^\top \boldsymbol{\gamma}} < ub_i$ **then**
    $\Delta\mu_i \leftarrow \Delta\mu_i + \gamma_i \frac{\Delta\mu(k)}{\mathbf{c}^\top \boldsymbol{\gamma}}$
  **end**
  utilizationRatio $\leftarrow \frac{\boldsymbol{\Delta\mu}^\top \mathbf{c}}{\Delta\mu_{\text{eq}}}$
**end**

Using the five hottest days each year for the years between 2051 and 2100, the performance of the PSO algorithm and the iterative metric-based method is compared in terms of the time taken and the values of the objective function. Sampling five representative days each year for a 50-year period gives 250 weather profiles, following the approach in [28], which provides the geographically explicit $\omega_i$ variables determining the failure probability of the network assets based on their location in the network/country. For each weather profile, five investment scenarios are considered, $\Delta\mu_{\text{eq}} \in [0.5, 1, 2, 4, 8]$. The amount of investment is formulated as the resources required to increase the design load for all assets in the network by $\Delta\mu_{\text{eq}}$. For the 1250 resulting combinations, it took the PSO algorithm 18291 s (approx. 5 h) to complete without parallelization with 8GB RAM, while the iterative metric-based method only took 855 s (approx. 15 min) to solve without parallelization and the same RAM availability. In addition to the realistic case study here presented, a comprehensive set of up to six-node synthetic networks is proposed in the electronic supplementary material, section S3 to evaluate the IRMA method in comparison with more established numerical techniques.

Figure 3 shows the value attained by the objective function using both methods against the amount of resource input. The objective function is the expected initial service disruption in the system when subjected to a given weather profile as a percentage of the service flow amount with no asset failures. The method concludes that a lower objective function value is considered optimum. From figure 3C, except $\Delta\mu_{\text{eq}} = 0$ with zero investment and $\Delta\mu_{\text{eq}} = 8$ with excessive investment, the proposed iterative metric-based method consistently gives an objective function that is smaller than the PSO algorithm when given the same amount of resources to distribute between assets.

The simulation suggests that the proposed iterative metric-based method can conclude better solutions in shorter computational time. We can compare how differently the two methods rank the assets to upgrade, figure 3B, where the correlation is expressed in terms of Kendall's $\tau - b$ coefficient.

In addition, we IRMA to two distinct collections of days. The first collection comprises the five hottest days each year for the year 2051–2100, *extreme days*. The second collection comprises 251 days selected using a clustering method, *typical days* [28]. For each day in a collection, we generate a solution using IRMA, which is averaged along each edge to give a combined solution, figure 4. From $\Delta\mu_{\text{eq}} = 0.5$ to $\Delta\mu_{\text{eq}} = 8$, with an increasing level of resource input, the amount of increase

Downloaded from https://royalsocietypublishing.org/ on 14 July 2025

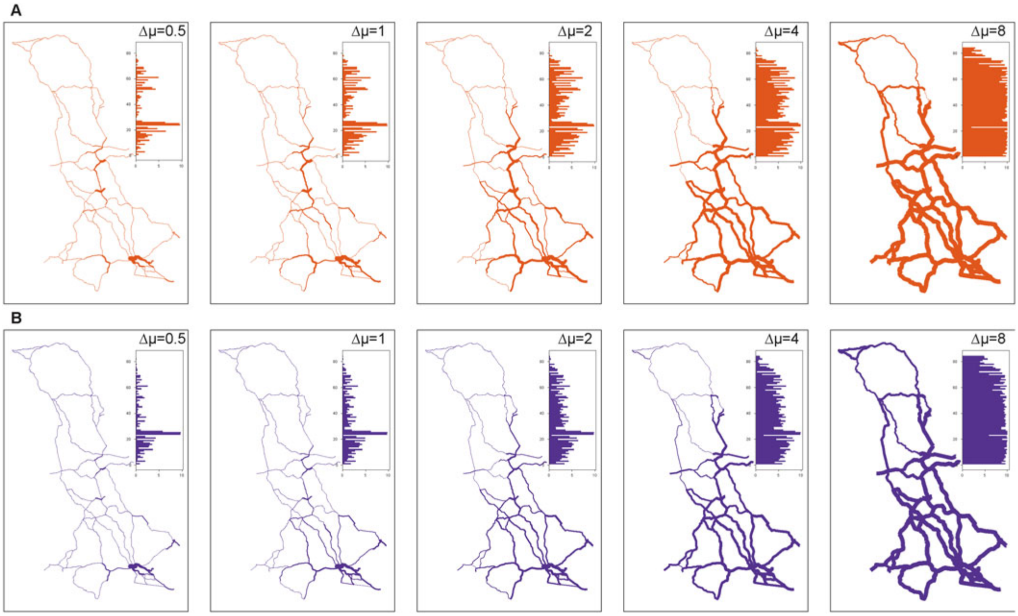


**Figure 4.** Maps showing the resource allocation solutions obtained from optimizing for extreme days (A) and for typical days (B) for different resource investment $\Delta\mu_{\rm eq}$. Width of the lines indicates the increment of allocated resource in increasing an asset's design load $\Delta\mu_i$. The insets show the distribution of $\Delta\mu_i$ against latitude for easier comparison of allocation homogeneity with increased resource availability.

in design load between edges gradually levels out, resulting in a decrease in the inequality in resource allocation. When resources are limited, concentrating them on fewer but more critical assets could be more beneficial rather than distributing the resources more widely.

## 5. Discussion

The requirement to adapt infrastructures to a changing climate stems from the lack of anticipation at the point of design on the conditions in which the assets would operate in a 50–100-year horizon [28]. This involves both the design features of single assets (e.g. the design capacity of drainage channels or, as in this case, the rail assembly to minimize thermal expansion) and the network design (e.g. the availability of alternative paths). Our results are limited to asset-wise interventions only, yet the outcome improves the overall network performance due to the use of system-wide metrics. In other words, the objective function, identified as a measure of the network throughput, is maximized through local interventions, to which resources are allocated in an optimal way. This is a centralized allocation, as one decided by a single decision-maker for the whole network. While this is the case for some infrastructure, it certainly is not universal. Large infrastructure systems are usually governed at regional level and are likely to be under multiple ownership [36,37]. For the railway network in Great Britain, the single owner and single decision maker scenario are quite realistic representations. This is also due to the insular nature of the land which is served by the infrastructure.

When multiple stakeholders are present, the optimal allocation problem is one of leveraging the competition or co-operation in the network in the strategic decisions about interventions. In this case, a spectral approach has been proposed where incentives are weighted according to the Perron vector associated to the network, hence highlighting the role of eigenvector centrality when competition dynamics [38], consensus dynamics [39] and possibly others, are considered.

Downloaded from https://royalsocietypublishing.org/ on 14 July 2025

In our static setting, the local marginal benefit constitutes a natural network ranking for resilience intervention. Assets can be easily ranked by the derivative of the benefit from the upgrade with respect to its cost. This recalls established results from linear programming as well as the literature just cited about the network spectral characteristics, considering the geometric interpretation of an eigenvector as the direction of maximum change. Noteworthy contributions to that are the extension to a network setting and the asset interdependence in ensuring the OD connectivity, hence the maximization of the expected throughput. Note also that, the results resonate with the fundamental works in resilience of complex systems [40], as resilience characteristics are mapped to a uni-dimensional variable, function of the local connectivity structure of the network, through a linearization of the network dynamics. In the same way, we connected a local metric to a global outcome, reducing the problem to a one-dimensional ranking.

The method is hence transparent in its formulation and yields results with immediate physical interpretation. As for its application to the Great Britain rail network, in addition to what has already been discussed about the suitability of the method, we shall note that the proposed resource allocation appears to prioritize highly connected and used parts of the network to then become more uniform as larger amounts of resources are available; see figure 4. Moreover, as more resources are available, their strategic allocation becomes less critical, with many possible allocations returning the minimization of the objective function. This is visible in figure 3, where the correlation between the PSO (heuristic) method and our proposed approach reduces when large upgrading resources become available (panels B and C). For limited available resources in figure 3C, the proposed method clearly outperforms the PSO algorithm, which is chosen as a benchmark in this case for its ability to mitigate the convergence to local minima via a multi-start procedure.

## 6. Conclusion

The upgrading of the infrastructure against threats of climate change can be tackled through investments in the network or in its operations. In this paper, we concentrated on the former, producing a resource allocation strategy that optimizes the expected network throughput. As different from many works in the literature on the subject, our network modelling included the flows, which entered directly in the objective function. This surpasses the resilience evaluation (and enhancement) based on the asset failures, focussing instead on the consequences for the service of the asset being unavailable. This results in an approach that, through local interventions, maximizes the traffic throughput as opposed to simply looking at the integrity of the paths. The proposed method uses original intuitions from linear programming mixed with an approach centred on the ranking of network elements, popular in the network science literature. The method surpasses numerical optimizers in terms of computational speed and flexibility, while retaining explanatory power due to its transparent formulation. This was verified through a case study on the Great Britain freight railway network, where the loss of service following an upgrade of the infrastructure is reduced by approximately 10% with respect to upgrading resources allocated using numerical optimization, while also significantly reducing the computational time.

Data accessibility. Supplementary material is available online [41].

Declaration of AI use. We have not used AI-assisted technologies in creating this article.

Authors' contributions. Q.L.: data curation, formal analysis, validation, writing—original draft; H.A.: conceptualization, methodology, visualization, writing—original draft, writing—review and editing; G.P.: conceptualization, methodology, validation, writing—original draft, writing—review and editing.

All authors gave final approval for publication and agreed to be held accountable for the work performed therein.

Conflict of interest declaration. We declare we have no competing interests.

Funding. No funding has been received for this article.

Downloaded from https://royalsocietypublishing.org/ on 14 July 2025

## References


1. Betts R, Haward A, Pearson K. 2021 The third UK climate change risk assessment. *Prepared for the Climate Change Committee, London*.
2. JCNSS TJCotNSS. 2022 Readiness for storms ahead? Critical national infrastructure in an age of climate change. Technical report, The House of Lords and the House of Commons.
3. Pörtner HO, Roberts DC, Adams H, Adler C, Aldunce P, Ali E, Begum RA, Betts R, Kerr RB, Biesbroek R *et al.* 2022 *Climate change 2022: impacts, adaptation and vulnerability*. Geneva, Switzerland: IPCC Geneva.
4. Treasury HM. 2020 National infrastructure strategy. Technical Report.
5. Treasury HM. 2021 Autumn budget and spending review 2021. Technical Report.
6. Administration B. 2022 *Building a better America—guidebook*. Whashington DC, USA.
7. Dawson RJ *et al.* 2018 A systems framework for national assessment of climate risks to infrastructure. *Phil. Trans. R. Soc. A* **376**, 20170298. (doi:10.1098/rsta.2017.0298)
8. Oehlers M, Fabian B. 2021 Graph metrics for network robustness—a survey. *Mathematics* **9**, 895. (doi:10.3390/math9080895)
9. Barabási AL. 2013 Network science. *Phil. Trans. R. Soc. A* **371**, 20120375. (doi:10.1098/rstb.2012.0375)
10. Freeman LC. 1977 A set of measures of centrality based on betweenness. *Sociometry* **40**, 35–41. (doi:10.2307/3033543)
11. Watts DJ, Strogatz SH. 1998 Collective dynamics of 'small-world' networks. *Nature* **393**, 440–442. (doi:10.1038/30918)
12. Edwards B, Hofmeyr S, Stelle G, Forrest S. 2012 Internet topology over time. (https://arxiv.org/abs/1202.3993).
13. Cadini F, Zio E, Petrescu CA. 2009 Using centrality measures to rank the importance of the components of a complex network infrastructure. In *Critical Information Infrastructure Security: 3rd Int. Workshop, CRITIS 2008, Rome, Italy, October13–15, 2008. Revised Papers 3*, pp. 155–167. New York, NY: Springer.
14. Zio E, Piccinelli R. 2010 Randomized flow model and centrality measure for electrical power transmission network analysis. *Reliab. Eng. Syst. Saf.* **95**, 379–385. (doi:10.1016/j.ress.2009.11.008)
15. Dunn S, Wilkinson SM. 2013 Identifying critical components in infrastructure networks using network topology. *J. Infrastruct. Syst.* **19**, 157–165. (doi:10.1061/(ASCE)IS.1943-555X.0000120)
16. Giustolisi O, Ridolfi L, Simone A. 2019 Tailoring centrality metrics for water distribution networks. *Water Resour. Res.* **55**, 2348–2369. (doi:10.1029/2018WR023966)
17. Hickish B, Fletcher DI, Harrison RF. 2019 A rail network performance metric to capture passenger experience. *J. Rail Transp. Plan. Manage.* **11**, 100138.
18. Hickish B, Fletcher DI, Harrison RF. 2022 A methodology to optimise a rail network specification for maximum passenger satisfaction and reduced initial investment. *J. Rail Transp. Plann. Manage.* **21**, 100279. (doi:10.1016/j.jrtpm.2021.100279)
19. Barrena E, Canca D, Coelho LC, Laporte G. 2014 Exact formulations and algorithm for the train timetabling problem with dynamic demand. *Comput. Oper. Res.* **44**, 66–74. (doi:10.1016/j.cor.2013.11.003)
20. Yin J, Yang L, Tang T, Gao Z, Ran B. 2017 Dynamic passenger demand oriented metro train scheduling with energy-efficiency and waiting time minimization: mixed-integer linear programming approaches. *Transp. Res. B: Methodol.* **97**, 182–213. (doi:10.1016/j.trb.2017.01.001)
21. Högdahl J, Bohlin M, Fröidh O. 2019 A combined simulation-optimization approach for minimizing travel time and delays in railway timetables. *Transp. Res. B: Methodol.* **126**, 192–212. (doi:10.1016/j.trb.2019.04.003)
22. Chakroborty P, Agarwal PK, Das A. 2012 Comprehensive pavement maintenance strategies for road networks through optimal allocation of resources. *Transp. Plann. Technol.* **35**, 317–339. (doi:10.1080/03081060.2012.671044)
23. Sun J, Balakrishnan S, Zhang Z. 2021 A resource allocation framework for predisaster resilience management of interdependent infrastructure networks. *Built Environ. Proj. Asset Manage.* **11**, 284–303. (doi:10.1108/BEPAM-06-2020-0109)
24. Lobban H, Almoghathawi Y, Morshedlou N, Barker K. 2021 Community vulnerability perspective on robust protection planning in interdependent infrastructure networks. *Proc. Inst. Mech. Eng. O* **235**, 798–813. (doi:10.1177/1748006X21991038)

25. McCarter M, Barker K, Johansson J, Ramirez-Marquez JE. 2018 A bi-objective formulation for robust defense strategies in multi-commodity networks. *Reliab. Eng. Syst. Saf.* **176**, 154–161. (doi:10.1016/j.ress.2018.04.011)
26. Fang YP, Zio E. 2019 An adaptive robust framework for the optimization of the resilience of interdependent infrastructures under natural hazards. *Eur. J. Oper. Res.* **276**, 1119–1136. (doi:10.1016/j.ejor.2019.01.052)
27. Poulin C, Kane MB. 2021 Infrastructure resilience curves: performance measures and summary metrics. *Reliab. Eng. Syst. Saf.* **216**, 107926. (doi:10.1016/j.ress.2021.107926)
28. Li Q, Punzo G, Robson C, Arbabi H, Mayfield M. 2024 A Systematic Approach to Climate Resilience Assessment of Infrastructure Networks. *IEEE Syst. J.* **18**, 24–35. (doi:10.1109/JSYST.2023.3329765)
29. National Infrastructure Commission. 2020 Anticipate, react, recover. Resilient infrastructure systems. Technical report, National Infrastructure Commission.
30. Berkeley AR, Wallace M, Coo C. 2010 A framework for establishing critical infrastructure resilience goals. *Final report and recommendations by the council, national infrastructure advisory council*, pp. 18–21.
31. Bruneau M, Chang SE, Eguchi RT, Lee GC, O'Rourke TD, Reinhorn AM, Shinozuka M, Tierney K, Wallace WA, Von Winterfeldt D. 2003 A framework to quantitatively assess and enhance the seismic resilience of communities. *Earthq. Spectra* **19**, 733–752. (doi:10.1193/1.1623497)
32. Sasidharan M, Burrow M, Ghataora G. 2020 A whole life cycle approach under uncertainty for economically justifiable ballasted railway track maintenance. *Res. Transp. Econ.* **80**, 100815 (doi:10.1016/j.retrec.2020.100815)
33. Palin EJ, Thornton HE, Mathison CT, McCarthy RE, Clark RT, Dora J. 2013 Future projections of temperature-related climate change impacts on the railway network of Great Britain. *Clim. Change* **120**, 71–93. (doi:10.1007/s10584-013-0810-8)
34. Kish A, Samavedam G. 2013 Track buckling prevention: theory, safety concepts, and applications. Technical report, John A. Volpe National Transportation Systems Center (US).
35. Network Rail. 2017 Freight network study. Technical Report.
36. Punzo G, Tewari A, Butans E, Vasile M, Purvis A, Mayfield M, Varga L. 2020 Engineering resilient complex systems: the necessary shift toward complexity science. *IEEE Syst. J.* **14**, 3865–3874. (doi:10.1109/JSYST.2019.2958829)
37. Cedergren A, Johansson J, Hassel H. 2018 Challenges to critical infrastructure resilience in an institutionally fragmented setting. *Safety Sci.* **110**, 51–58. (doi:10.1016/j.ssci.2017.12.025)
38. Galeotti A, Golub B, Goyal S. 2020 Targeting interventions in networks. *Econometrica* **88**, 2445–2471. (doi:10.3982/ECTA16173)
39. Punzo G, Young GF, Macdonald M, Leonard NE. 2016 Using network dynamical influence to drive consensus. *Sci. Rep.* **6**, 26318. (doi:10.1038/srep26318)
40. Gao J, Barzel B, Barabási AL. 2016 Universal resilience patterns in complex networks. *Nature* **530**, 307–312. (doi:10.1038/nature16948)
41. Li Q, Arbabi H, Punzo G. 2025 An emergent optimal resource allocation for climate resilience of transport infrastructure networks. Figshare. (doi:10.6084/m9.figshare.c.7879893)

Downloaded from https://royalsocietypublishing.org/ on 14 July 2025